Human Molecular Genetics, 2014, Vol. 23, No. 6 **1631–1643**
doi:10.1093/hmg/ddt555
Advance Access published on November 7, 2013

Dual-tagged amyloid-β precursor protein reveals distinct transport pathways of its N- and C-terminal fragments

Christine Villegas, Virgil Muresan and Zoia Ladescu Muresan*

Department of Pharmacology and Physiology, New Jersey Medical School, Rutgers, The State University of New Jersey, Newark, NJ 07101-1709, USA

Received August 16, 2013; Revised October 29, 2013; Accepted October 30, 2013

The amyloid-β precursor protein (APP), a type I transmembrane protein genetically associated with Alzheimer's disease, has a complex biology that includes proteolytic processing into potentially toxic fragments, extensive trafficking and multiple, yet poorly-defined functions. We recently proposed that a significant fraction of APP is proteolytically cleaved in the neuronal soma into N- and C-terminal fragments (NTFs and CTFs), which then target independently of each other to separate destinations in the cell. Here, we prove this concept with live imaging and immunolocalization of two dual, N- and C-termini-tagged APP constructs: CFP-APP-YFP [containing the fluorescent tags, cyan fluorescent protein (CFP) and yellow fluorescent protein (YFP)] and FLAG-APP-Myc. When expressed at low levels in neuronal cells, these constructs are processed into differently tagged NTFs and CTFs that reveal distinct distributions and characteristics of transport. Like the endogenous N- and C-terminal epitopes of APP, the FLAG-tagged NTFs are present in trains of vesicles and tubules that localize to short filaments, which often immunostain for acetylated tubulin, whereas the Myc-tagged CTFs are detected on randomly distributed vesicle-like structures. The experimental treatments that selectively destabilize the acetylated microtubules abrogate the distribution of NTFs along filaments, without altering the random distribution of CTFs. These results indicate that the NTFs and CTFs are recruited to distinct transport pathways and reach separate destinations in neurons, where they likely accomplish functions independent of the parental, full-length APP. They also point to a compartment associated with acetylated microtubules in the neuronal soma—not the neurite terminals—as a major site of APP cleavage, and segregation of NTFs from CTFs.

INTRODUCTION

The amyloid-β precursor protein (APP), a ubiquitously expressed, type I transmembrane protein, is considered to be at the core of Alzheimer's disease (AD) pathology (1). In neurons, APP is transported along cytoskeletal tracks—microtubules, and, occasionally, actin filaments—to the sites of its presumed functions within the cell soma and the neuronal processes (2,3). The molecular mechanisms underlying this transport are not understood (4). This is explained by the complex biology of APP, which includes proteolytic processing into fragments (Fig. 1A) that could have separate fates (2,3,5). The proteolytic processing affects only a fraction of total APP and can occur in multiple intracellular compartments (6–11). We recently proposed that, in neurons, the cleavage of APP largely occurs in the cell soma and that each type of APP fragment is transported independently to specific but different destinations within the neurites (2,12). This idea emerged from immunolocalization studies with antibodies recognizing epitopes from different domains of APP, which showed that the N- and C-terminal domains are detected in separate transport entities and accumulate at distinct sites in neurites. While this result is consistent with separate transport of APP N- and C-terminal fragments (NTFs and CTFs) rather than transport of full-length APP (2), one could argue that steric hindrance and epitope masking by interacting proteins could prevent the detection of certain epitopes in certain cellular contexts. To unambiguously track and evaluate the relative localization of NTFs and CTFs, we expressed dual, N- and

*To whom correspondence should be addressed at: Department of Pharmacology and Physiology, New Jersey Medical School, Rutgers, The State University of New Jersey, 185 South Orange Avenue, MSB, I-665, Newark, NJ 07101-1709, USA. Tel: +973 9724385; Fax: +973 9727950; Email: zoia.muresan@njms.rutgers.edu

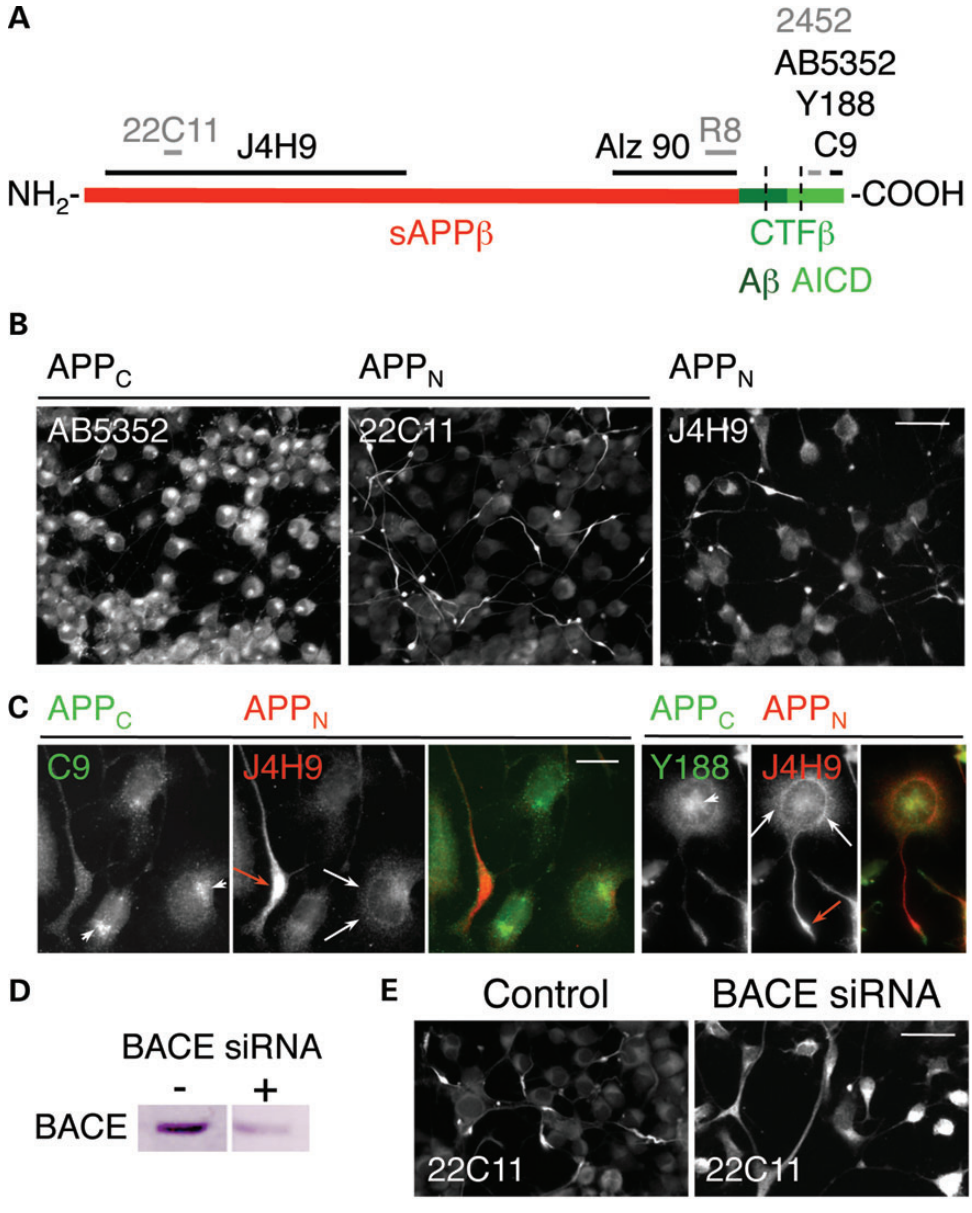

Figure 1. C-terminal (APP_C) and N-terminal (APP_N) epitopes of APP show distinct distributions in the soma and associate with different transport carriers within the neurites. (**A**) Schematic diagram of APP^{695} showing the positions of epitopes recognized by antibodies raised to APP polypeptides (black and gray lines) used in this study. Different colors mark the positions of the polypeptides generated from cleavage of APP by β-secretase (sAPPβ and CTFβ) and γ-secretase (the amyloid-β peptide, Aβ and the APP intracellular domain, AICD). The segment between dotted lines indicates the position of the transmembrane domain. (**B** and **C**) CAD cells were immunolabeled with antibodies to the cytoplasmic domain (AB5352, C9 or Y188) and the ectodomain (22C11 or J4H9) of APP. Red arrows in (C) show accumulation of N-terminal epitopes at the neurite terminals; arrowheads show accumulation of C-terminal epitopes at a compact region in the soma; white arrows show localization of N-terminal epitopes to a compartment tightly associated with, and surrounding, the nucleus. Quantitatively, only 22 ± 5% (mean ± SD) of the detected C-terminal epitopes were localized to neurites, compared with 59 ± 9% of the N-terminal epitopes ($P < 0.005$). (**D** and **E**) Silencing BACE with siRNA in CAD cells reduces BACE levels with >75% (D) and diminishes accumulation of N-terminal epitopes in the distal neurites by ∼50% (28 ± 4% localized to neurites; $P < 0.01$), detected with antibody 22C11 (E). Scale bars, 50 μm (B and E) and 20 μm (C).

C-termini-tagged APP (CFP-APP-YFP and FLAG-APP-Myc) in neuronal cells and studied the distribution of the tags. While the N- and C-termini of APP often co-localize, they also clearly show non-overlapping localization to particulate structures with distinct distributions along cytoskeletal tracks, when expressed at low levels in neuronal cells with flat neurites. These results are in accord with the idea of extensive APP processing in the neuronal soma and segregated transport of APP-derived fragments within neuronal processes.

RESULTS

N- and C-terminal epitopes of endogenous APP are segregated in the soma and the neurites

In a previous study done with antibodies recognizing different domains of APP, we found striking, non-overlapping distribution of N- and C-terminal epitopes within neuronal cells—CAD cells and cortical neurons—in culture and *in situ* (2). These results were extended here with additional antibodies

recognizing epitopes from the cytoplasmic region, or the ectodomain, of APP (Fig. 1B and C, and Supplementary Material, Fig. S1). In the cell soma, in addition to some co-localization, the N- and C-terminal epitopes also appear segregated, a situation that suggests the presence of cleaved and separately sorted fragments. While the C-terminal epitopes mostly localize to a compact region in the vicinity of the nucleus, the N-terminal epitopes are primarily detected in an extended compartment tightly associated with, and surrounding, the nucleus (Fig. 1C, and Supplementary Material, Fig. S1B; see specificity controls in Supplementary Material, Fig. S1). These results support the notion that the cell soma is a major site of APP processing, and generation of NTFs and CTFs. Of note is the preferential accumulation of NTFs at neurite terminals, compared with CTFs (Fig. 1B and C). This accumulation is significantly abolished upon silencing the expression of beta-site APP-cleaving enzyme 1 (BACE1; the major β-secretase), the protease responsible for the generation of a large fraction of NTFs and CTFs (Fig. 1D and E). Concomitantly, the co-localization of the immunodetected N- and C-terminal epitopes of APP along the processes increases with >20% ($P < 0.02$), confirming the previously reported, increased transport of full-length APP into neurites upon blocking the activity of β-secretase (5). Taken together, these results indicate that, while full-length APP is transported into neurites along with the fragments, the accumulation at neurite terminals is a characteristic of NTFs, rather than intact APP. Proximity ligation assays (PLA), described later, also support this notion (see Supplementary Material, Fig. S7). With CAD cell extracts, we found that the blot region usually attributed to immature and mature full-length APP also contains co-migrating, bona fide NTFs, primarily the product of β-secretase cleavage, soluble APP-β (sAPPβ) (Fig. 2A–C). Many studies erroneously assumed that this region in blots only contains full-length APP species. Yet, as our study now reveals, NTFs are present at detectable levels within neurons under normal conditions.

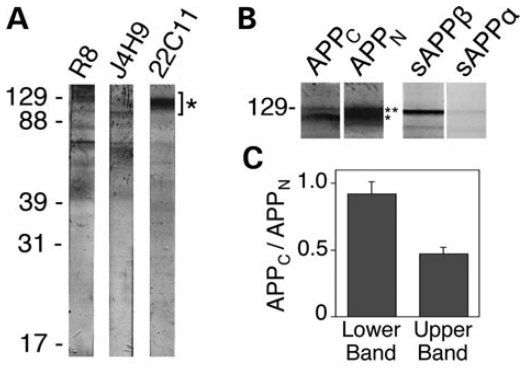

Figure 2. APP-derived NTFs reside within neurons. (**A**) Immunoblot analysis of CAD cell extracts with antibodies raised against polypeptides from the ectodomain of APP (see Fig. 1A for location of the recognized epitopes). Full-length APP species migrate to positions indicated by (*). All antibodies also detect polypeptides of lower molecular size; as many of these additional bands are detected by all antibodies, they likely are bona fide cleavage products of APP or sAPP. The position of molecular size markers (in kDa) is shown at left. (**B**) Immunoblots of CAD cell extracts with antibodies to polypeptides from the C-terminal (APP_C) and N-terminal (APP_N; 22C11) regions of APP, and with antibodies detecting the free C-termini of sAPPβ or sAPPα, which do not cross-react with full-length APP. Note that CAD cell extracts contain genuine sAPPβ, which co-migrates with full-length APP species. Notably, under our SDS–PAGE conditions, sAPPβ has a lower electrophoretic mobility compared with the immature APP species, but higher than the mature, full-length APP. (**C**) Histogram, derived from western blots, showing the ratios of the staining intensities with the antibodies to APP_C and APP_N (APP_C/APP_N) for the lower (*) and upper (**) bands in the APP region (see B). Note that the ratios differ significantly and indicate that the upper band includes APP species that contain the N-terminal epitope, but lack the C-terminal epitope. The histogram indicates that approximately half of the staining with antibody 22C11 in the upper band may represent high molecular size NTFs, such as sAPPβ. Bars represent SD.

APP-derived NTFs, but not CTFs, show a peculiar, filamentous distribution, rather than a discrete, vesicular distribution, along cytoskeletal filaments

We examined the distribution of N- and C-terminal epitopes of APP within the neurites in more detail. As previously reported (2), these are largely segregated to distinct transport carriers. Interestingly, the C-terminal epitopes appear associated with randomly distributed, vesicle-like structures (Fig. 3A and B), whereas the N-terminal epitopes are often detected as elongated structures—possibly trains of closely spaced vesicles or tubular transport entities—which distribute strictly along defined filamentous tracks (Fig. 3C). The filament-like labeling pattern is particularly evident in the soma and proximal neurites of enlarged, flattened CAD cells (Fig. 3C), and in the growth cones of extending neurites (Fig. 3B). The N-terminal epitopes of APP strictly delineate filamentous tracks throughout the neurites, including the very thin ones; this is clearly seen in the varicosities (Supplementary Material, Fig. S2A). Occasionally, the distribution of the N-terminal epitopes appears limited to one or two filaments, usually in the central region of the process (Fig. 3C). The filament-like distribution is detected with several antibodies recognizing different epitopes within the ectodomain of APP (Fig. 3C; see Fig. 1A for the location of the recognized epitopes), as well as with antibodies detecting the free C-terminus of sAPPβ (Fig. 3D). Hence, it is unlikely that the antibodies cross-react with cytoskeleton-associated proteins, unrelated to APP. No filamentous distribution is seen with antibodies to the amyloid precursor-like protein 2 (APLP2), a protein related to APP that also undergoes cleavage by secretases (13,14), or in $APP^{-/-}$ neuronal cells, which express both APLP1 and APLP2 (Supplementary Material, Fig. S3). Importantly, the filament-like distribution of the N-terminal epitopes of APP is significantly diminished in CAD cells transfected with BACE1 siRNA (Supplementary Material, Fig. S2B), a condition that largely prevents the proteolytic cleavage of APP. Topologically, the cleaved NTFs should reside inside membrane-bounded compartments. This is confirmed by the lack of immunolabeling with antibodies to the APP ectodomain in CAD cells treated with saponin, prior to formaldehyde fixation, and omission of the Triton X-100 extraction step, usually done after fixation (Supplementary Material, Fig. S4). These results show that the observed tight association with cytoskeletal tracks is typical for NTFs, not full-length APP. They also indicate that the transport of NTFs and CTFs implicates not only their segregation with different carriers, but also distinct transport routes and, most likely, distinct regulatory mechanisms. This point is further supported by the dependence of intracellular distribution of APP C-terminal, but not N-terminal epitopes, on the level of expression of Fe65, a scaffolding protein with potential role in the transport of APP (4). As exemplified in Supplementary Material,

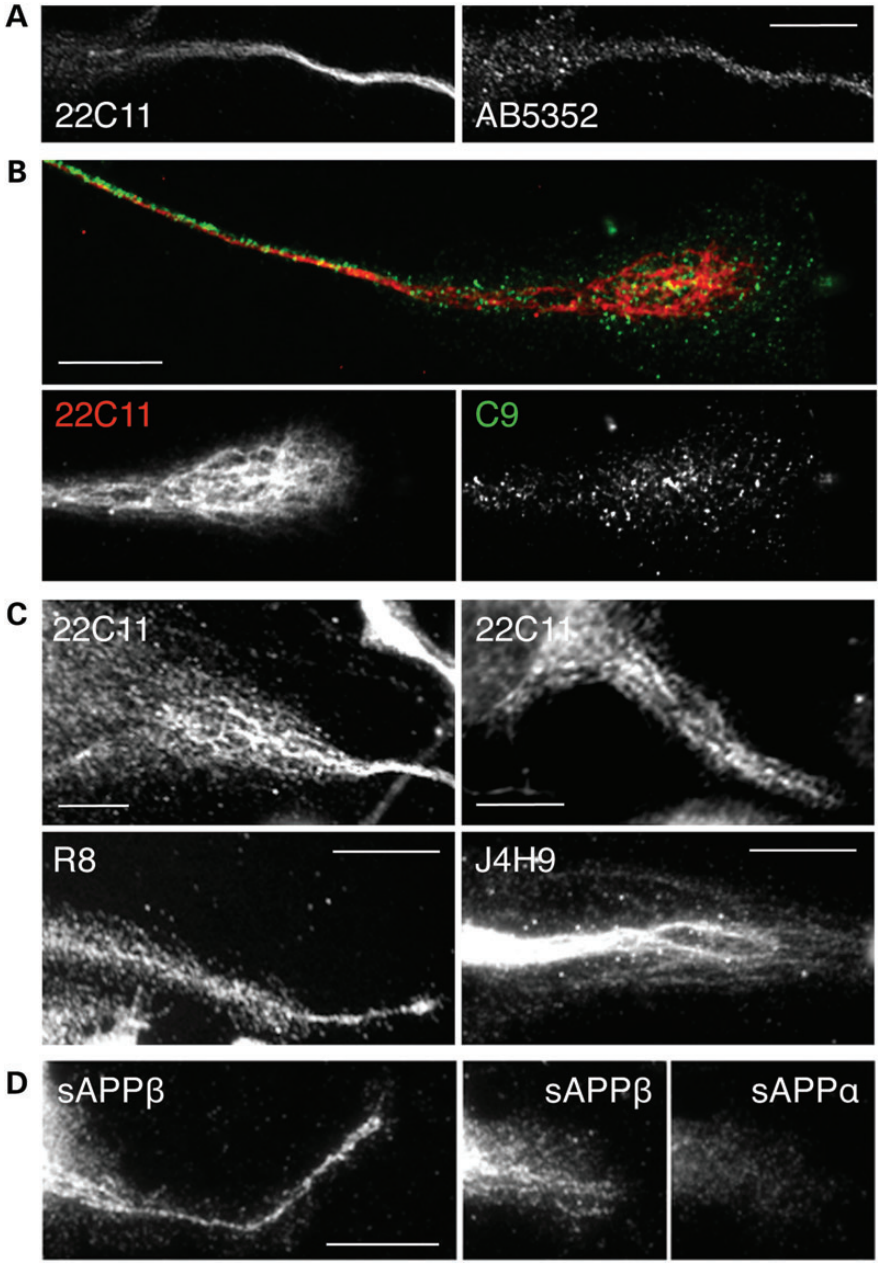

Figure 3. APP-derived NTFs strictly localize to cytoskeletal filaments in CAD cells. (**A**–**C**) The labeling obtained with monoclonal (22C11, J4H9) and polyclonal (R8) antibodies, recognizing epitopes in the N-terminal region of APP (see Fig. 1A for location of epitopes), reveals a typical, filamentary distribution pattern, clearly detectable in flattened regions of the cell (C), including the growth cone (B). In contrast, antibodies recognizing C-terminal epitopes (AB5352, C9) show a discrete, random distribution (right images in A and B). The grayscale images in (B) reproduce the growth cone shown in the upper image, at right. (**D**) Antibodies specific for the free C-terminal end of sAPPβ, but not sAPPα, show filamentary distribution. Occasionally, the labeling pattern with the anti-sAPPβ antibody strikingly resembles the distribution of mitochondria. Scale bars, 20 μm.

Figure S5A–C, the exogenous expression of Fe65 in CAD cells increases the accumulation of CTFs but not NTFs within neurites; when compared with controls, >55% of cells transfected with Fe65-Myc show increased levels of APP (immunolabeled with antibodies to its C-terminus) at terminals. Moderate expression of FLAG-tagged c-Jun NH_2-terminal kinase interacting protein-1 (JIP-1)—a manipulation that selectively perturbs the transport of phosphorylated APP and phosphorylated CTFs (15)—does not affect the neuritic levels, and the filamentous distribution, of N-terminal APP epitopes (Supplementary Material, Fig. 5D), consistent with the idea of distinct regulation of transport of NTFs and phosphorylated CTFs.

Given the requirement for kinesin-1 for the transport into neurites of APP and its fragments (7,15–18), it appeared likely that the filamentous distribution of NTFs was owing to an intimate association of the cargo with the microtubules; such

association is usually less evident for other kinesin-1 cargoes described in the literature but is reminiscent of the tight association of ATPase-deficient kinesin-1 mutants, stably attached to microtubules (19). The limited number of the NTF-positive tracks (Fig. 3) suggested that only a subfraction of microtubules is used for the transport of the NTFs. Microtubule heterogeneity within cells could arise from the various posttranslational modifications of the incorporated tubulin. Of the major classes of posttranslationally modified microtubules, those targeted by lysine acetylation of α-tubulin show the highest degree of co-localization with the N-terminal epitopes of APP (Fig. 4A and C), a result confirmed with a second anti-acetylated tubulin antibody that strictly recognizes K40-acetylated tubulin (20) (Fig. 4B). Interestingly, this antibody shows extensive co-localization with the N-terminal APP epitopes in the soma, as well as at the neurite terminals (Fig. 4B). We previously showed that acetylated microtubules are preferentially disrupted by cold methanol (21). Consistent with a possible association of the NTFs with acetylated microtubules, the treatment of CAD cells with cold methanol reduces both the localization at the perinuclear compartment, and the filament-like distribution, of APP N-terminal epitopes (Supplementary Material, Fig. S6). Notably, the distribution of C-terminal epitopes—and their distinct localization compared with N-terminal epitopes—is not affected by this treatment (Supplementary Material, Fig. S6B; compare with Fig. 1B and C). While treatment with cold methanol may have additional effects on the preservation of intracellular structures, taken together these results are consistent with the notion that the NTFs, but not the CTFs, are preferentially associated with acetylated microtubules in neurons.

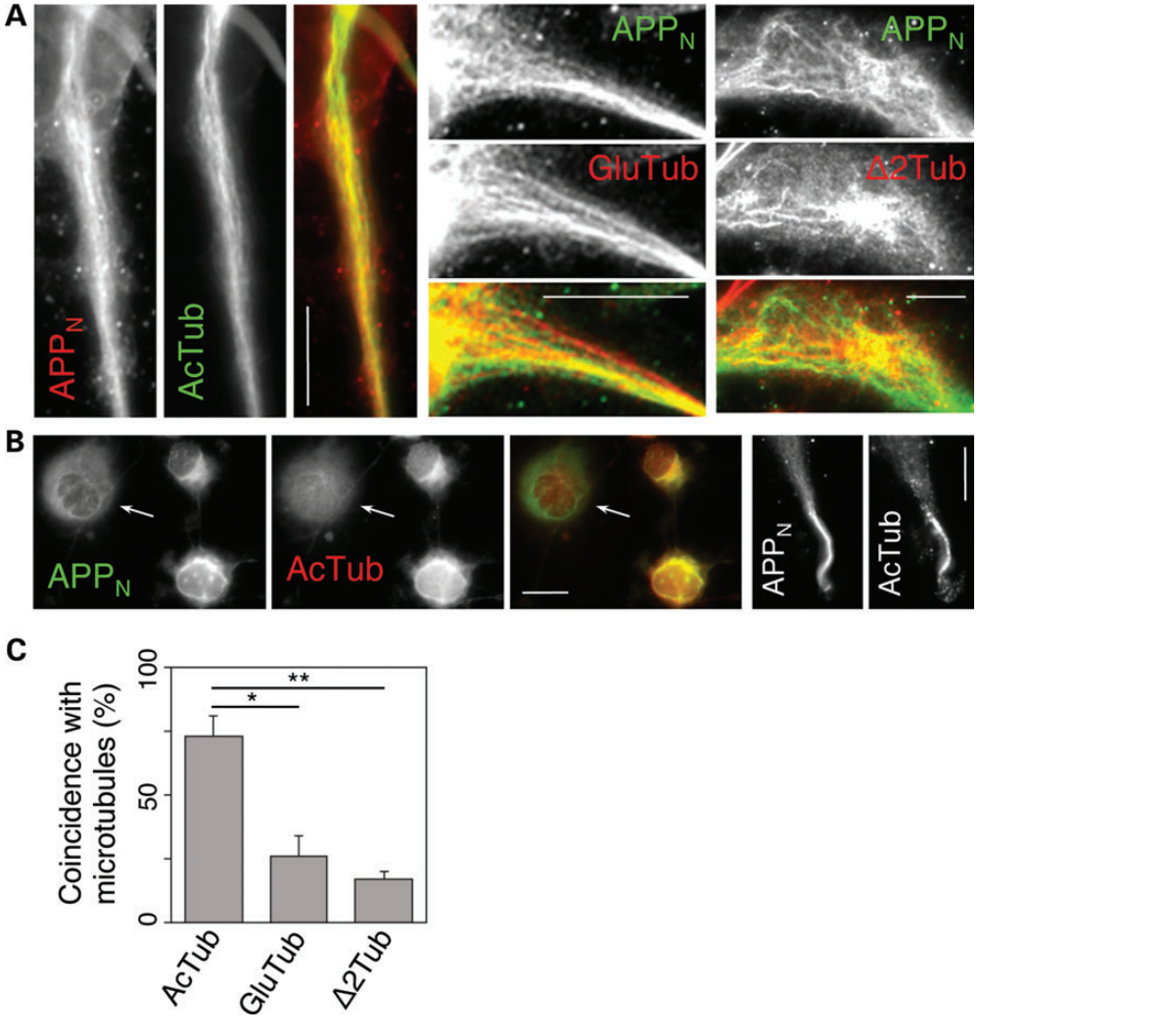

Figure 4. The NTFs of APP primarily associate with acetylated microtubules in CAD cells. (**A**) Significant co-localization of APP N-terminal epitopes (APP_N; detected with antibody 22C11) with acetylated microtubules (AcTub; detected with monoclonal antibody 611B1), but not with detyrosinated (GluTub) or delta 2-tubulin (Δ2Tub) microtubules. (**B**) Extensive co-localization of APP_N with acetylated microtubules (detected with polyclonal anti-acetyl-K40 antibody) in the soma, as well as at the neurite terminals. Note that the perinuclear accumulation of NTFs is largely diminished in the cell lacking a perinuclear network of acetylated microtubules (arrow). Scale bars, 20 μm. (**C**) Quantitative analysis of co-localization of APP_N with microtubules showing different posttranslational modification. In spite of a high cell-to-cell variability, the coincidence of the 22C11 immunolabeled filaments with AcTub is significantly higher than that with GluTub (* indicates $P < 0.01$) or Δ2Tub (** indicates $P < 0.001$). Bars represent SEM.

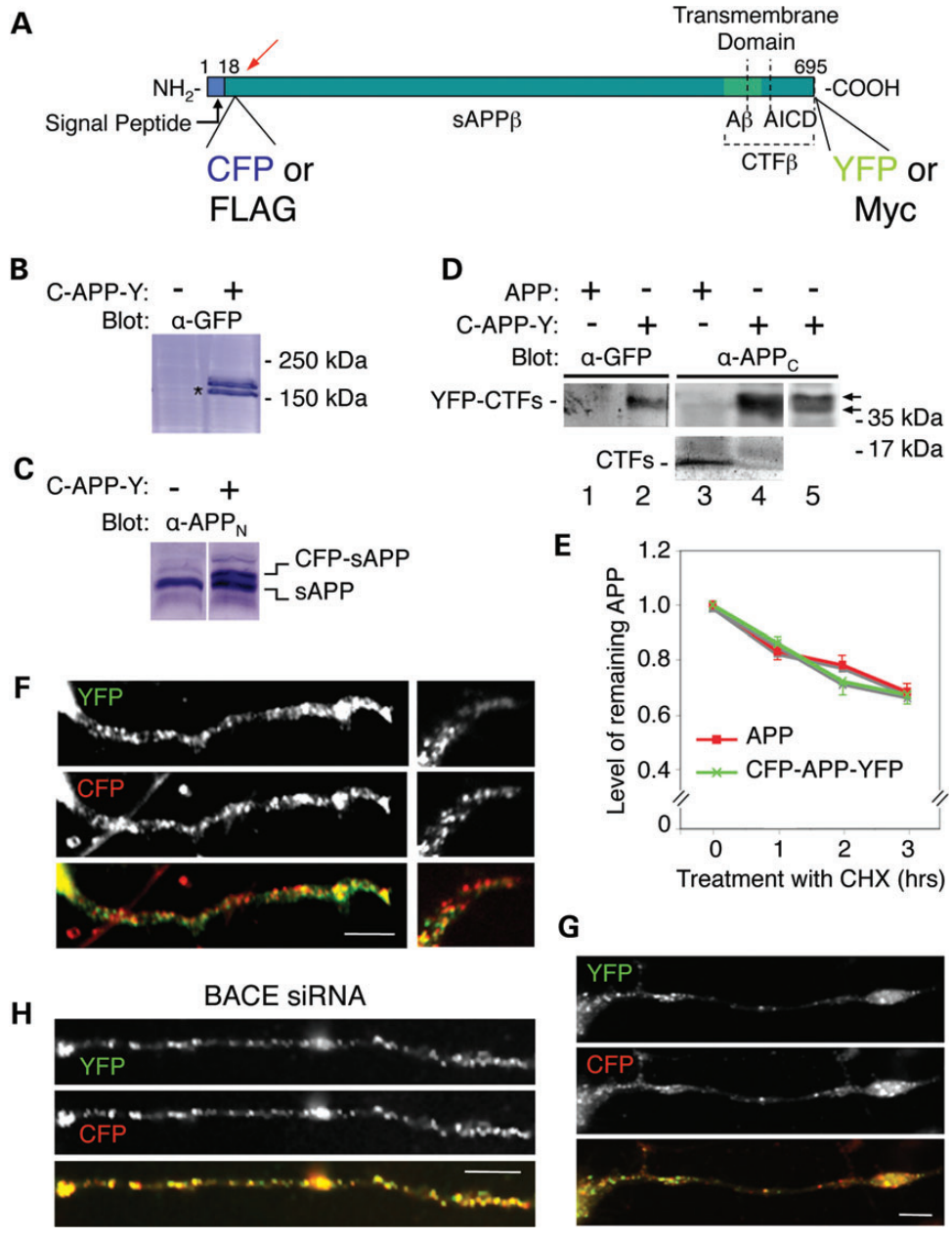

Figure 5. N- and C-terminal tags of exogenously expressed APP show both co-localization and segregated distribution within neurites. (**A**) Drawing of the CFP-APP-YFP and FLAG-APP-Myc constructs, showing position of tags, and sites of cleavage of APP via the β/γ-secretase pathway, which produces sAPPβ, CTFβ, Aβ and AICD. (**B**) Expression of CFP-APP-YFP (C-APP-Y) in CAD cells. A GFP blot of extracts of CAD cells, transfected or not with dual-tagged APP, is shown. The N-terminally, CFP-tagged sAPP band, detected below the CFP-APP-YFP band, is indicated by (*). (**C**) CFP-sAPP is secreted into the medium. A blot, done with antibody 22C11 (detecting an APP N-terminal epitope, APP_N), of culture media from CAD cells transfected or not with CFP-APP-YFP is shown. (**D**) CFP-APP-YFP, or untagged APP, expressed in HEK293 cells are cleaved and generate YFP-tagged CTFs (upper lanes) or untagged CTFs (bottom lanes), as revealed with antibodies against GFP or the C-terminal region of APP (α-APP_C). The two YFP-CTFs (α and β), not resolved in lanes 2 and 4, are clearly seen in lane 5 (arrows). (**E**) Similar decay of CFP-APP-YFP and APP, after blocking protein synthesis with cycloheximide (CHX). APP levels at the beginning of CHX treatment were set to 1.0. Bars represent SEM. At each time point, the difference between the decay of CFP-APP-YFP and APP was not significant ($P < 0.5$). (**F** and **G**) Partial segregation of CFP (N-terminus of APP, shown in red color) from YFP (C-terminus, shown in green color) in the neurites of CAD cells expressing CFP-APP-YFP at low level. Images were obtained from live, unfixed cultures. Note that the N-terminal tag often—but not always—accumulates more distally than the C-terminal tag (G, and right images in F). (**H**) Increased co-localization of CFP with YFP in neurites of CAD cells transfected with CFP-APP-YFP and BACE siRNA (compare with F and G). Quantitatively, the down-regulation of BACE1 with siRNA in CAD cells to <25% leads to ~25% increase ($P < 0.005$) in the number of vesicles that carry both the CFP and YFP tag (likely containing full-length APP), compared with controls. Specifically, 63 ± 2% (mean ± SEM) of the CFP-containing vesicles detected in neurites also contained YFP in cells transfected with BACE siRNA, compared with 45 ± 3% in controls. Quantitative analysis was done in CAD cells that expressed CFP-APP-YFP at low levels. Scale bars, 10 μm.

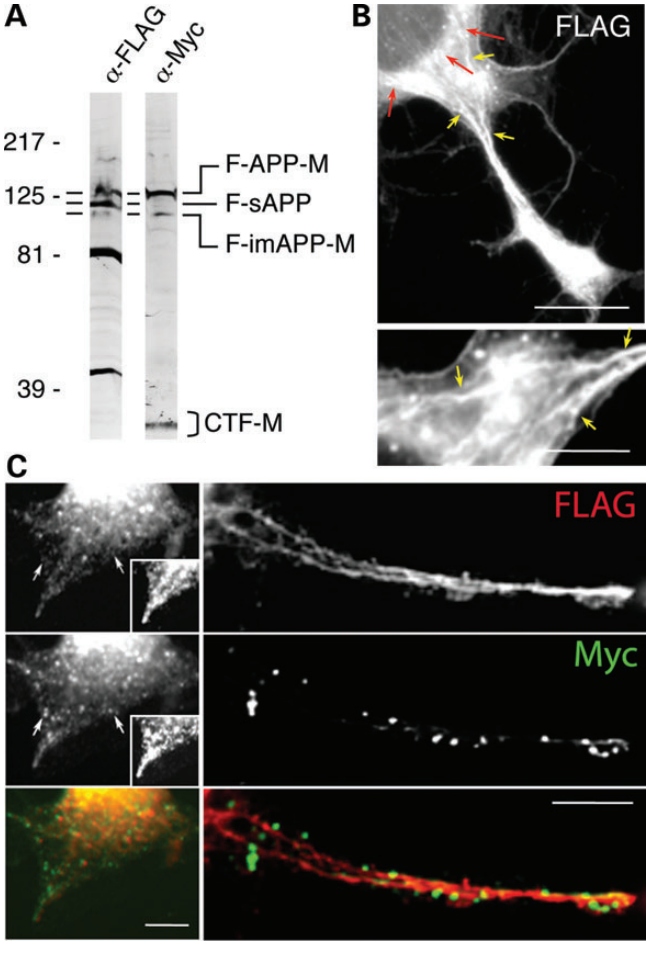

Figure 6. N-terminal, but not C-terminal tags of exogenously expressed APP show intimate association with cytoskeletal tracks. (**A**) Exogenously expressed FLAG-APP-Myc (F-APP-M) is processed into known N- and C-terminal APP fragments. Cleavage of F-APP-M by β-secretase generates the NTF, sAPP, which contains only the FLAG tag (F-sAPP), and the CTF, which contains only the Myc tag (CTF-M). Immature APP contains both tags (F-imAPP-M). Similar to the endogenous APP, the mature, extensively glycosylated F-APP-M has a lower electrophoretic mobility than F-imAPP-M, which is less glycosylated. Also similar to endogenous sAPP, the F-sAPP migrates in SDS–PAGE at a position situated between F-imAPP-M and F-APP-M. We note that the small FLAG and Myc tags do not detectably alter the molecular size of the dual-tagged APP and the cleaved fragments. The band at ∼40 kDa, detected only with the anti-FLAG antibody, likely represents a previously described N-terminal fragment of APP (55). An additional band at ∼80 kDa is also detected. As antibodies to the N-terminal region of APP also detect a band of this size in non-transfected cells (see Fig. 2), it likely represents a bona fide NTF. The wavy appearance of the band corresponding to F-APP-M (α-FLAG blot, at left) is likely due to a gel irregularity. The short, horizontal bars at the left side of the blots point to corresponding bands. (**B** and **C**) The FLAG tag, but not Myc tag, distributes along clearly identifiable filamentous tracks in CAD cells transfected with FLAG-APP-Myc. Note that the Myc tag shows a discrete, vesicle-like distribution, whereas the FLAG tag reveals a quasi-continuous filamentary distribution, likely attributable to trains of vesicles and membrane tubules (C). Red arrows in (B) point to the perinuclear region where FLAG-tagged NTFs reside in the soma. Also note the accumulation of FLAG-tagged NTFs at the process terminal, similar to the accumulation of N-terminal epitopes of endogenous APP. The bottom image in (B) reproduces at higher magnification an area of the upper image, showing part of the soma and the proximal neurite; the image is rotated left 90°. The extensive, filamentous distribution of the FLAG tag is clearly visible. Yellow arrows point to corresponding sites in the two images. Insets in (C) reproduce the process shown in the left images at increased contrast, to allow clear evaluation of the distinct distribution of the two tags. Similar distribution patterns were detected in three separate experiments. The filamentous distribution of the FLAG tag was consistently detected only within flattened soma and neurites of cells expressing the dual-tagged APP at low levels, which represented ∼10% of the transfected cells. No filamentous distribution of the Myc tag was detected in these experiments. Scale bars, 20 μm (upper image in B); 10 μm (C, and lower image in B).

The distributions of N- and C-terminal tags of exogenously expressed APP highlight distinct transport pathways for APP, NTFs and CTFs within the neurites

To directly test whether the NTFs and CTFs of APP segregate with distinct transport vesicles, we employed CAD cells expressing the APP construct, CFP-APP-YFP, containing different fluorescent tags at its termini: the cyan fluorescent protein (CFP) inserted close to the N-terminus, and the yellow fluorescent protein (YFP) fused in frame to the C-terminus of APP (Fig. 5A). The CFP-APP-YFP protein, when expressed at low levels, lacks toxicity and reiterates the biology of endogenous APP in terms of posttranslational processing, decay, intracellular localization and compatibility with neuronal differentiation. Indeed, at low levels of expression, the dual-tagged APP—clearly identifiable in immunoblotting and cytochemistry—is proteolytically cleaved to generate similar proportions of sAPPs (which are NTFs) and CTFs (Fig. 5B–D); the rate of decay upon cyclohexymide treatment—which blocks protein synthesis—is similar to that of endogenous APP (Fig. 5E). Thus, the dual-tagged APP—at low levels of expression—is a reliable reporter for APP processing and targeting. CAD cells transfected with CFP-APP-YFP were examined by fluorescence imaging of CFP and YFP in live cells. As previously reported for exogenously expressed, untagged or C-terminally tagged APP (APP-YFP), we find extensive co-localization of CFP and YFP in CAD cells expressing CFP-APP-YFP at high levels, when the dual-tagged APP uncharacteristically penetrates the filopodia-like processes that emanate laterally from the main neuronal process (Supplementary Material, Fig. S7A). In these cases, the C-terminal tag, YFP, massively accumulates at neurite terminals, which is atypical for the C-terminal epitopes of endogenous APP (see Fig. 1). However, in cells expressing low levels of CFP-APP-YFP, the two tags segregate in part to different vesicles within neurites (Fig. 5F and G). In such cases, the distribution of the N-terminal tag, CFP, mostly mimics the distribution of immunoreactivity detected with antibodies raised to N-terminal APP epitopes (Supplementary Material, Fig. S7B), and the C-terminal tag seldom accumulates at the neurite terminal (Supplementary Material, Fig. S7C), as is characteristic for the endogenous C-terminal epitopes (see Fig. 1). This segregation is largely dependent on the activity of β-secretase, because—as in the case of N- and C-terminal epitopes of endogenous APP—it is significantly abolished upon silencing BACE1 expression with siRNA (Fig. 5H). We note that the co-localization of the two fluorescent tags—when detected—could also, at least in part, represent co-localization of CTFs with NTFs, rather than the presence of uncleaved full-length APP. It is also conceivable that mixtures of full-length APP, NTFs and CTFs are present in the same location, a possibility that is supported by the different CFP/YFP ratios detected in different parts of the transfected cells (Supplementary Material, Fig. S7C).

Imaging studies of APP tagged with fluorescent proteins were complemented by experiments with dual-tagged APP, carrying

smaller tags: FLAG, at its N-terminal end, and Myc, at its C-terminus (Fig. 5A). Upon expression in CAD cells, FLAG-APP-Myc is subjected to cleavage by secretases, as confirmed with immunoblot detection of the tagged NTFs and CTFs (Fig. 6A). Immunocytochemistry with antibodies recognizing the tags was used to localize the termini of the dual-tagged FLAG-APP-Myc, or single-tagged FLAG-NTF and CTF-Myc polypeptides. As with the fluorescently tagged APP constructs, at high level of expression of FLAG-APP-Myc in CAD cells, the FLAG and Myc tags co-localize extensively. However, at low expression levels (a condition that is achieved in ∼10% of the transfected cells), significant segregation of the two tags is detected within the neurites. Remarkably, within flattened neurites, the FLAG tag (marking the N-terminus of APP), but not the Myc tag (C-terminus), distributes along filamentous tracks in a pattern similar to that of the N-terminal epitopes of endogenous APP (Fig. 6B and C). Also similar to the endogenous N-terminal epitopes, in the soma, the FLAG tag concentrates in a perinuclear region (Fig. 6B, upper image). The filamentous distribution of the FLAG tag is detected in ∼10% of the transfected cells with flattened neurites. This frequency is similar to the frequency of cells that express FLAG-APP-Myc at low levels, which confirms again that, at high level of expression, transport of APP proceeds differently than at normal endogenous levels. We also note that the filamentous distribution is easily missed in cells with small rounded soma. This situation is similar to the detectability of the filamentous, microtubule network in cultured neurons, which can only be observed in cells with flattened soma and neurites. The filamentous distribution of the N-terminal tag is not apparent with the CFP-APP-YFP construct, possibly because of the large size of the fluorescent tag, CFP. In conclusion, the live imaging and immunocytochemistry data of dual-tagged APP in neurons, like the immunocytochemistry data of endogenous APP epitopes, reveal transport pathways of the NTFs and CTFs that are distinct of each other, and of the full-length APP (Fig. 7).

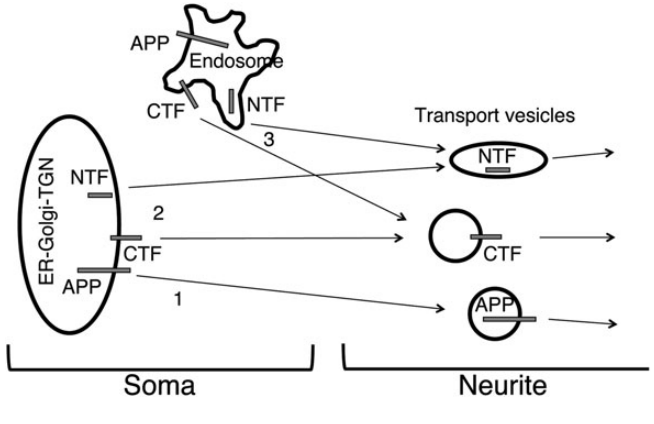

Figure 7. Schematic diagram showing three possible trafficking pathways of APP: (1) transport of full-length APP; (2,3) independent transport of cleaved NTFs and CTFs of APP, segregated into distinct membrane-bounded carriers. The transport carriers originate from either the early secretory compartments, including the ER/ERGIC and the TGN (2), or endosomes in the soma (3). NTFs are depicted inside elongated structures, as they appear in immunocytochemistry.

DISCUSSION

The elucidation of the molecular mechanisms of transport of APP in neurons has been a constant preoccupation of researchers since the discovery that the metabolism of APP, including its processing by secretases, is intimately related to its intracellular trafficking. Here we identify the neuronal soma as a major site of generation—and segregation—of NTFs and CTFs. The nature of the compartments in the soma where the NTFs and CTFs segregate and accumulate was not addressed in this study and remains to be established. In the case of the NTFs, this compartment has a perinuclear distribution and co-localizes with neurofilaments (12) and acetylated microtubules, and its integrity depends on the integrity of both the neurofilaments (12) and the acetylated microtubules (this study). The CTFs accumulate at a compact, pericentrosomal compartment that co-localizes extensively with markers for the ER–Golgi intermediate compartment (ERGIC), the trans-Golgi-network (TGN) and the endosomal recycling compartment (ERC) (unpublished results), which roughly localize to the same region of the cell (22). While all three compartments are sites where APP cleavage could occur (9,23–27), a probable scenario is that CTFs accumulate at the ERC, after being generated in early endocytic compartments from cell surface-retrieved APP. Indeed, results of PLA, done with neurons expressing FLAG-APP-Myc, are consistent with the presence of full-length APP in subplasmalemmal compartments—a typical location for early endosomes—present in the soma and proximal–medial neurites (Supplementary Material, Fig. S7E). We also find that a significantly larger fraction of the CTFs is retained in the cell body, compared with the NTFs; unlike the CTFs (5), the NTFs appear to be massively exported from the soma into the neurites. Using immunocytochemistry with multiple antibodies that detect epitopes in the ecto- and the endo-domain of APP, we have confirmed and extended our previous findings that suggest separate transport and segregated localization of NTFs and CTFs within the neurites.

Because of the complex biology of APP, which includes intricate posttranslational modification and interaction with numerous proteins, tracing transport and localization of APP and of its derived fragments is a difficult, almost insurmountable task, with the current methodology. As the exogenous expression of APP could affect its proper folding, and alter the regulation and rate of its posttranslational modifications (including its phosphorylation and cleavage by secretases), and could perturb its interactions with the proteins that regulate its transport and metabolism, we initially opted to extract information on APP transport from the localization of the endogenous APP along its transport routes (2,15); this is a powerful strategy also adopted by other groups studying APP transport (28). This approach overwhelmingly suggested that APP is—to a significant extent—transported into neurites as cleaved fragments resulted from proteolytic processing in the neuronal soma. However, immunocytochemistry, even when performed with a large number of validated antibodies specifically recognizing different regions of APP, as we did, has limitations due, for example, to steric hindrance, epitope masking, cross-reactivity with other proteins and sensitivity to fixation. We therefore complemented the inquiries of endogenous APP with studies of exogenously expressed APP, carrying different tags at its N- and C-termini. To allow for direct comparison with data of immunocytochemistry of the

endogenous APP, we monitored the localization of the tags rather than their transport. We note that the combined, complementary use of immunocytochemistry of endogenous proteins with the localization of the tags of expressed, tagged proteins is currently considered the best approach for studying protein localization (29). Using imaging of CFP-APP-YFP in live cells, and immunocytochemistry with anti-tag antibodies (in FLAG-APP-Myc expressing cells), we confirmed the partially segregated distribution of APP's N- and C-termini within the neurites, in neurons that express the dual-tagged APP al low levels, a result consistent with segregated transport of the NTFs and CTFs. We also confirmed reports from our and other laboratories (2,30) showing that, at moderate-to-high levels of expression (a frequent situation in transfected cells), the two tags largely co-localize, both in the cell soma and in the neurites. While the co-localization of the tags could indicate the presence of full-length APP, it does not rule out the possibility that some NTFs and CTFs, generated in the soma, are transported together, with the same vesicles. Discerning between these two possibilities will not be easy; both the FRET (for CFP-APP-YFP) and PLA (for FLAG-APP-Myc) analysis are insufficiently tested for transmembrane proteins, where the two epitopes reside on opposite sites of the membrane, and their separation could easily exceed the distance over which FRET can occur. In the case of PLA, detection relies on the physical interaction of the two DNA strands of the PLA probes (each attached via the primary antibodies to the tested epitopes), which could be blocked by the interposing membrane proteins. Our attempts to test for proximity of the FLAG and Myc tags in CAD cells transfected with FLAG-APP-Myc occasionally produced PLA signals, possibly revealing the location at steady state of full-length APP. As stated earlier, the distribution of the signal was present at intracellular sites consistent with organelles of the early secretory pathway—ER, ERGIC, Golgi—and, in particular, early endosomes, adjacent to the plasma membrane (Supplementary Material, Fig. S7E). While these are expected locations for full-length APP, one cannot exclude the possibility that cleaved fragments do co-exist with APP. Taken together, these results confirm the segregated transport into neurites of NTFs and CTFs, but also indicate that, at high levels of expression, the machineries of APP processing and/or segregation of the cleaved fragments could be overwhelmed and dysregulated. This is a general matter of concern in all cases where a protein, extensively involved in interactions with other proteins, is expressed at levels that exceed the binding capacity of the endogenous interacting proteins (31).

In our study, the presence of the tags did not grossly alter the processing of APP by secretases, as shown by the immunoblot detection of APP-derived fragments at the expected electrophoretic mobility, according to the known cleavage pattern of APP by secretases. In addition to the bona fide sAPPs and CTFs, we also detected two prominent, FLAG-tagged NTFs. As their molecular size is smaller than that of sAPP, it is likely that they are further cleavage products of sAPP. We note that polypeptides smaller than sAPP were also detected with the antibodies to the APP ectodomain in non-transfected cells, suggesting that APP and sAPP may undergo additional proteolytic processing inside neurons.

An important result of this study is the identification of a tight association of the NTF-containing compartments with cytoskeletal tracks along the neurites. Interestingly, a tight association of APP (detected with antibodies to its ectodomain) with cytoskeletal filaments was reported in early, pioneering studies of APP localization (32,33), but those findings have not been followed up. While association with the microtubules is anticipated for any cargo transported by kinesins, the peculiar, filamentous distribution of the NTFs is striking—not normally seen with other kinesin cargoes—and suggests that the transport of NTFs, unlike that of CTFs, could occur either as trains of vesicles or tubular structures, such as tubular transport vesicles, tubular endosomes, ER extensions or mitochondria-associated membrane compartments. Considering that proteins localizing to the cytoskeleton show unusually low correlation between localization observed with immunocytochemistry and protein tagging (29), the fact that the filamentous distribution of the N-terminal region of APP was detected for both endogenous APP and exogenously expressed, tagged APP (FLAG-APP-Myc) is remarkable. This reliably indicates that the mechanism of transport of the NTFs is fundamentally different than that of the CTFs. This conclusion is also supported by the dependence on the APP-binding protein, Fe65, of the transport into neurites of CTFs, but not of NTFs, as well as the association of NTFs, but not CTFs, with acetylated microtubules.

The idea that the APP-derived polypeptides have themselves functional significance for the homeostasis of the neuron is not new (3). However, it was mostly assumed that their function is tightly linked to the full-length APP and that the cleavage of APP and the generation of the fragments occur at the sites where they function. Our results showing that the site of the generation of the fragments is different from the site(s) where they accumulate, combined with the separate transport of the different fragments to different destinations within the neuron, are consistent with the idea that APP exerts its functions, at least in part, through its cleavage products. Thus, the functions of the fragments could be independent of each other, and distinct from that of full-length APP. In this scenario, APP is just the precursor of a set of polypeptides that have functions unrelated to each other or to the parental protein. This idea remains to be explored in future studies.

MATERIALS AND METHODS

Antibodies

Antibodies recognizing domains in sAPP (N-terminal epitopes): mouse anti-APP, MAB348 (clone 22C11; epitope, residues 66–81; Millipore–Chemicon, Billerica, MA, USA); mouse anti-APP, MBS200099 (clone J4H9; immunogen, residues 18–289; MyBiosource, San Diego, CA, USA); rabbit anti-APP, R8 (immunogen, residues 628–652; gift of Dr Nikos Robakis, Mount Sinai School of Medicine, New York, NY, USA); mouse anti-Alz 90 (MAB349; raised against a synthetic peptide corresponding to amino acids 511–608 of APP pre-A4695; Millipore–Chemicon); mouse anti-sAPPα, 11088 (clone 2B3; does not cross-react with full-length APP or sAPPβ; IBL, Gunma, Japan); rabbit anti-sAPPβ, 18857 (does not cross-react with full-length APP or sAPPα; IBL). Antibodies recognizing C-terminal epitopes of APP: rabbit monoclonal anti-APP, 1565-1 (clone Y188; immunogen, peptide from the NPTY region; Epitomics, Burlingame, CA, USA); rabbit

anti-APP, AB5352 (immunogen, nine amino acid peptides from the C-terminus; Millipore–Chemicon); rabbit anti-APP, C9 (immunogen, residues 676–695; gift of Dr Dennis Selkoe, Brigham and Women's Hospital, Boston, MA, USA); rabbit anti-APP, 2452 (immunogen, peptide corresponding to residues surrounding Thr^{668}; Cell Signaling Technology, Danvers, MA, USA). Other antibodies: rabbit anti-APLP2 [anti-D2-II, raised against full-length mouse APLP2; does not cross-react with APP and APLP1 (13); Millipore–EMD–Calbiochem, La Jolla, CA, USA]; rabbit anti-BACE, M-83 (Santa Cruz Biotechnology, Santa Cruz, CA, USA); mouse anti-acetylated tubulin (6-11B-1) [Sigma Chemical Co., St. Louis, MO, USA; this antibody recognizes both acetylated and recently de-acetylated, but not non-acetylated microtubules (20)]; rabbit anti-acetyl-K40, raised against an acetylated peptide corresponding to the primary sequence of mouse α-tubulin [gift of Dr Kristen Verhey, University of Michigan, Ann Arbor, MI, USA; this antibody strictly recognizes acetylated microtubules in cells (20)]; rabbit anti-detyrosinated tubulin (Glu-tubulin) and rabbit anti-delta 2 tubulin (Millipore); mouse anti-green fluorescent protein (GFP) (IL-8, BD Living Colors™; cross-reacts with YFP; used in immunoblotting); mouse anti-c-Myc, Ab-1 (clone 9E10; Oncogene Research Products, San Diego, CA, USA); fluorescein-labeled chicken anti-c-Myc antibody (affinity purified; Aves Labs, Inc., Tigard, OR, USA); mouse anti-DDK (4C5; detects the FLAG epitope; Origene Technologies, Rockville, MD, USA); rabbit anti-FLAG (F7425, affinity purified; Sigma).

Plasmids

The CFP-APP-YFP expression plasmid was obtained starting from APP-YFP (gift of Dr Carlos Dotti and Dr Christoph Kaether, European Molecular Biology Laboratory, Heidelberg, Germany) inserted into pcDNA3, with YFP ligated in front of the stop codon of human APP^{695} (17). CFP was introduced in frame, immediately after the nucleotide sequence encoding the 17-amino acid signal peptide of APP that targets the N-terminus of the fusion protein into the ER membrane (Fig. 5A). The FLAG-APP-Myc construct was obtained by mutagenesis starting from the expression plasmid encoding untagged human APP^{695} in pcDNA3 (gift of Dr Li-Huei Tsai, The Picower Institute for Learning and Memory, MIT, Howard Hughes Medical Institute, Cambridge, MA, USA); it also contains a tetracysteine motif (Cys_4) (34) in tandem with the N-terminal FLAG tag (not shown in Fig. 5A), a feature that was not used in this study. JIP-1-FLAG (35) was a gift of Dr Roger Davis (University of Massachusetts Medical School, Howard Hughes Medical Institute, Boston, MA, USA). Fe65-Myc (36) was a gift of Dr Ben Margolis (University of Michigan, Howard Hughes Medical Institute, Ann Arbor, MI, USA).

Cell cultures and transfections

Mouse CNS-derived CAD cells (37) were grown in 1:1 F12/DME medium, containing 8% fetal bovine serum and penicillin/streptomycin. Differentiation was induced by culturing cells in the absence of serum (37). CAD cells, originating from the locus coeruleus, have been successfully employed by us and by others in many studies related to AD or other neurological disorders (38–45). We note that recent studies point to neurons of the locus coeruleus as a site where both oligomerization of Aβ and aggregation of tau could be initiated in AD (42,46–48). In addition, a proposed revision of the stages of AD, known as Braak stages (49), now includes the brainstem as the site where the AD brain pathology begins (46,47). Thus, CAD cells are highly relevant to AD. $APP^{-/-}$ neuronal cells (gift of Dr Man-Sun Sy and Dr Shin-Cheng Kang, Case Western Reserve University, Cleveland, OH, USA) were grown under standard conditions (50,51). HEK293 cells were grown in RPMI 1640 containing 8% serum. Transfection of cells with CFP-APP-YFP, FLAG-APP-Myc or JIP-1-FLAG was performed using Nucleofector technology (Lonza—Amaxa, Walkersville, MD, USA) (15). The low level of expression of the dual-tagged APP constructs—judged by the absence of the tags from the filopodia-like processes that emanate laterally from the soma and neurites—was critical for observing segregation of the tags, especially in the case of CFP-APP-YFP. For exogenous expression of Fe65, CAD cells were transfected with Fe65-myc together with GFP. For RNAi treatment, CAD cells were transfected with siRNA duplexes specific for mouse BACE1 (Santa Cruz Biotechnology). Transfected cells were allowed to attach to the coverslip in the presence of serum and then cultured for 24–48 h in the absence of serum, to induce differentiation. To analyze the decay of APP and CFP-APP-YFP, parallel cultures of HEK293 cells, non-transfected (expressing endogenous APP) or transfected with either wild-type APP or CFP-APP-YFP, were treated with 100 μg/ml cycloheximide (to block protein synthesis) for 1, 2 or 3 h. Cells were collected and analyzed for APP or CFP-APP-YFP by quantitation of immunoblots. No difference between the decay of endogenous APP, transfected wild-type APP, or transfected CFP-APP-YFP was detected.

Immunoblotting and immunocytochemistry

Differentiated CAD cells were rinsed twice with phosphate-buffered saline (PBS) and extracted in SDS sample buffer, 5 min at 95°C. Extracts were analyzed for the presence of APP and APP-derived polypeptides (NTFs and CTFs), BACE1, FLAG, Myc or GFP by western blotting of transfers to polyvinylidene difluoride membrane (52). Protein loads in sample and control lanes were compared by Ponceau S staining prior to immunoblotting. Band intensities in blots were quantified using the NIH ImageJ64 software.

For immunocytochemistry, CAD cells were fixed (PBS, containing 4% formaldehyde, 4% sucrose), permeabilized (0.3% Triton X-100) and processed for single or dual antigen labeling as described elsewhere (2). Occasionally, cells were fixed by immersion of coverslips in dry ice-chilled methanol for 5 min and stored in PBS until immunostaining. Among others, this procedure efficiently disrupts acetylated microtubules (21). To permeabilize cells without affecting intracellular membranes, we treated cultures with 0.02% saponin prior to formaldehyde fixation (53), omitting the postfixation, lipid extraction step with Triton X-100. Secondary antibodies coupled to Alexa dyes (488 and 594) were from Invitrogen-Molecular Probes. Nonspecific binding of secondary antibodies was assessed in experiments that omitted the primary antibodies. Specificity of antibodies, raised against C-terminal epitopes of APP, for their

cognate epitopes was verified in control experiments that used incubation of the specimens in the presence of competing polypeptide used at 100:1 molar excess over IgG (2). We used a polypeptide that encompassed a 12-amino acid region centered on Thr^{668} in the APP cytoplasmic domain (termed here 'short APP_C polypeptide') and a biotinylated polypeptide encompassing the entire APP cytoplasmic domain (termed here 'long APP_C polypeptide') (2). Antibodies to the ectodomain of APP (e.g. antibody 22C11) were pre-adsorbed on a membrane that contained the APP region of an overloaded transfer of rat brain extract (to remove the anti-APP immunoreactive species from the IgG fraction), or pre-adsorbed on a membrane that contained transferred BSA (2).

Fluorescently tagged proteins (CFP-APP-YFP and GFP) were detected via the intrinsic fluorescence of the tags, using CFP-, YFP- and GFP-specific filters. For co-localization studies of the YFP and CFP tags, checking for alignment in the two fluorescence channels was essential. This was confirmed by the perfect superposition of the images obtained through the two channels in CAD cells expressing pmaxGFP (Lonza—Amaxa), the fluorescence of which is detectable through both the YFP and the CFP channel (Supplementary Material, Fig. S7D).

In situ proximity ligation assay (PLA) to test for proximity of the tagged N- and C-termini of APP, in CAD cells transfected with FLAG-APP-Myc, was done with the Duolink kit (Olink Bioscience, Uppsala, Sweden), according to the manufacturer's instructions, using mouse anti-Myc (PLA probe MINUS) and rabbit anti-FLAG (PLA probe PLUS) as primary antibodies. Controls for specificity included absence of primary antibodies, or the use of only one primary antibody.

Image acquisition and processing

Images were acquired with an Olympus IX81 microscope (Tokyo, Japan) equipped with Semrock, Inc. filters (Rochester, NY, USA), cooled CCD camera (Hamamatsu Photonics, Hamamatsu City, Japan) and Image-Pro Plus software (Media Cybernetics, Rockville, MD, USA). The images were processed for contrast and brightness with Adobe Photoshop (Adobe Systems, Inc.). Occasionally, the distribution of fluorescent particles along neurites was analyzed in thresholded, inverted, gray-scale images, using the NIH ImageJ64 software (43).

For co-localization studies, the extent of co-localization of two epitopes was estimated by quantifying percent coincidence of fluorescent particles between two channels, as described elsewhere (43). This procedure provides a better quantitation of particle co-localization than the percentage of pixel overlap between the two channels. Co-localization of NTFs with defined types of microtubules was assessed by quantifying the extent of coincidence of the 22C11 immunolabeled filaments with the microtubules, detected with antibodies to the different posttranslationally modified tubulins.

Statistical analysis

Statistical analysis to determine significance between experimental groups was done using a two-sample *t*-test for the two-tailed hypothesis (54). For each experimental condition, data were derived from at least two separate experiments.

The fraction of Fe65-myc/GFP transfected cells that showed increased immunostaining at neurite terminals with antibodies to the N- or C-terminal regions of APP (detected in the red channel) was determined as follows. First, an exposure time was selected so that only ~20% of non-transfected cells showed detectable fluorescence labeling in the neurites (in the red channel). Using this exposure time, images were acquired throughout the coverslip, moving from one field to the next. Only a fraction of cells showed immunolabeling. Duplicate images were acquired in the green channel, with exposures that allowed detection of all GFP expressing cells. The percentage of GFP expressing cells that also stained for the APP C (or N)-terminus (above the selected threshold) was calculated.

AUTHOR CONTRIBUTION

Z.L.M. conceived, designed and coordinated the study, generated the dual-tagged APP constructs and performed most experiments. C.V. performed immunoblotting and immunocytochemistry. V.M. performed live imaging and immunocytochemistry. All authors analyzed and interpreted the results. Z.L.M. and V.M. wrote the manuscript, with contributions from C.V.

SUPPLEMENTARY MATERIAL

Supplementary Material is available at HMG online.

ACKNOWLEDGEMENTS

We thank Dr Nikos Robakis, Dr Denis Selkoe and Dr Kristen Verhey for kindly providing antibodies; Dr Roger Davis, Dr Carlos Dotti, Dr Christoph Kaether, Dr Ben Margolis and Dr Li-Huei Tsai for kindly providing cDNA constructs; Dr Dona Chikaraishi and Dr James Wang for kindly providing the CAD cells and Dr Man-Sun Sy and Dr Shin-Cheng Kang for kindly providing the $APP^{-/-}$ neuronal cells.

Conflict of Interest statement. None declared.

FUNDING

This work was supported by National Institutes of Health (AG039668 to Z.L.M.); National Science Foundation (IOS-1347090 to V.M. and Z.L.M.); and University of Medicine and Dentistry of New Jersey Foundation (grant to Z.L.M. and V.M.).

REFERENCES

1. Bettens, K., Sleegers, K. and Van Broeckhoven, C. (2013) Genetic insights in Alzheimer's disease. *Lancet Neurol.*, **12**, 92–104.
2. Muresan, V., Varvel, N.H., Lamb, B.T. and Muresan, Z. (2009) The cleavage products of amyloid-β precursor protein are sorted to distinct carrier vesicles that are independently transported within neurites. *J. Neurosci.*, **29**, 3565–3578. PMCID: PMC2669751.
3. Zheng, H. and Koo, E.H. (2011) Biology and pathophysiology of the amyloid precursor protein. *Mol. Neurodegener.*, **6**, 27.
4. Muresan, V. and Muresan, Z. (2009) Is abnormal axonal transport a cause, a contributing factor or a consequence of the neuronal pathology in Alzheimer's disease? *Future Neurol.*, **4**, 761–773. PMCID: PMC2805861.

5. Rodrigues, E.M., Weissmiller, A.M. and Goldstein, L.S. (2012) Enhanced beta-secretase processing alters APP axonal transport and leads to axonal defects. *Hum. Mol. Genet.*, **21**, 4587–4601.
6. De Strooper, B. and Annaert, W. (2000) Proteolytic processing and cell biological functions of the amyloid precursor protein. *J. Cell Sci.*, **113**, 1857–1870.
7. Kamal, A., Almenar-Queralt, A., LeBlanc, J.F., Roberts, E.A. and Goldstein, L.S.B. (2001) Kinesin-mediated axonal transport of a membrane compartment containing beta-secretase and presenilin-1 requires APP. *Nature*, **414**, 643–648.
8. Vetrivel, K.S. and Thinakaran, G. (2006) Amyloidogenic processing of beta-amyloid precursor protein in intracellular compartments. *Neurology*, **66**, S69–S73.
9. Willnow, T.E. and Andersen, O.M. (2013) Sorting receptor SORLA—a trafficking path to avoid Alzheimer disease. *J. Cell Sci.*, **126**, 2751–2760.
10. Wilson, C.A., Doms, R.W., Zheng, H. and Lee, V.M. (2002) Presenilins are not required for Abeta42 production in the early secretory pathway. *Nat. Neurosci.*, **5**, 849–855.
11. Yu, W.H., Cuervo, A.M., Kumar, A., Peterhoff, C.M., Schmidt, S.D., Lee, J.H., Mohan, P.S., Mercken, M., Farmery, M.R., Tjernberg, L.O. *et al.* (2005) Macroautophagy—a novel Beta-amyloid peptide-generating pathway activated in Alzheimer's disease. *J. Cell Biol.*, **171**, 87–98.
12. Muresan, V., Villegas, C. and Ladescu Muresan, Z. (2013) Functional interaction between amyloid-beta precursor protein and peripherin neurofilaments: a shared pathway leading to Alzheimer's disease and amyotrophic lateral sclerosis? *Neuro-degener. Dis.*, DOI: 10.1159/000354238.
13. Thinakaran, G., Kitt, C.A., Roskams, A.J., Slunt, H.H., Masliah, E., von Koch, C., Ginsberg, S.D., Ronnett, G.V., Reed, R.R., Price, D.L. *et al.* (1995) Distribution of an APP homolog, APLP2, in the mouse olfactory system: a potential role for APLP2 in axogenesis. *J. Neurosci.*, **15**, 6314–6326.
14. Walsh, D.M., Minogue, A.M., Sala Frigerio, C., Fadeeva, J.V., Wasco, W. and Selkoe, D.J. (2007) The APP family of proteins: similarities and differences. *Biochem. Soc. Trans.*, **35**, 416–420.
15. Muresan, Z. and Muresan, V. (2005) Coordinated transport of phosphorylated amyloid-beta precursor protein and c-Jun NH2-terminal kinase-interacting protein-1. *J. Cell Biol.*, **171**, 615–625. PMCID: PMC2171566.
16. Amaratunga, A., Leeman, S.E., Kosik, K.S. and Fine, R.E. (1995) Inhibition of kinesin synthesis in vivo inhibits the rapid transport of representative proteins for three transport vesicle classes into the axon. *J. Neurochem.*, **64**, 2374–2376.
17. Kaether, C., Skehel, P. and Dotti, C.G. (2000) Axonal membrane proteins are transported in distinct carriers: a two- color video microscopy study in cultured hippocampal neurons. *Mol. Biol. Cell*, **11**, 1213–1224.
18. Morfini, G., Quiroga, S., Rosa, A., Kosik, K. and Caceres, A. (1997) Suppression of KIF2 in PC12 cells alters the distribution of a growth cone nonsynaptic membrane receptor and inhibits neurite extension. *J. Cell Biol.*, **138**, 657–669.
19. Nakata, T. and Hirokawa, N. (1995) Point mutation of adenosine triphosphate-binding motif generated rigor kinesin that selectively blocks anterograde lysosome membrane transport. *J. Cell Biol.*, **131**, 1039–1053.
20. Soppina, V., Herbstman, J.F., Skiniotis, G. and Verhey, K.J. (2012) Luminal localization of alpha-tubulin K40 acetylation by cryo-EM analysis of fab-labeled microtubules. *PLoS ONE*, **7**, e48204.
21. Muresan, V. and Muresan, Z. (2009) In vitro reconstitution of dynamic, er-like, nanotubular networks, and of small, tubulo-vesicular transport entities by interactions of cytoplasmic dynein and spectrin with liposomes. *Biophys. J.*, **96**, 507a.
22. Puri, C., Renna, M., Bento, C.F., Moreau, K. and Rubinsztein, D.C. (2013) Diverse autophagosome membrane sources coalesce in recycling endosomes. *Cell*, **154**, 1285–1299.
23. Choy, R.W., Cheng, Z. and Schekman, R. (2012) Amyloid precursor protein (APP) traffics from the cell surface via endosomes for amyloid beta (Abeta) production in the trans-Golgi network. *Proc. Natl. Acad. Sci. USA*, **109**, E2077–E2082.
24. Cook, D.G., Forman, M.S., Sung, J.C., Leight, S., Kolson, D.L., Iwatsubo, T., Lee, V.M. and Doms, R.W. (1997) Alzheimer's A beta(1–42) is generated in the endoplasmic reticulum/intermediate compartment of NT2N cells. *Nat. Med.*, **3**, 1021–1023.
25. Refolo, L.M., Sambamurti, K., Efthimiopoulos, S., Pappolla, M.A. and Robakis, N.K. (1995) Evidence that secretase cleavage of cell surface Alzheimer amyloid precursor occurs after normal endocytic internalization. *J. Neurosci. Res.*, **40**, 694–706.
26. Sambamurti, K., Refolo, L.M., Shioi, J., Pappolla, M.A. and Robakis, N.K. (1992) The Alzheimer's amyloid precursor is cleaved intracellularly in the trans-Golgi network or in a post-Golgi compartment. *Ann. N. Y. Acad. Sci.*, **674**, 118–128.
27. Thinakaran, G. and Koo, E.H. (2008) Amyloid precursor protein trafficking, processing, and function. *J. Biol. Chem.*, **283**, 29615–29619.
28. Szpankowski, L., Encalada, S.E. and Goldstein, L.S. (2012) Subpixel colocalization reveals amyloid precursor protein-dependent kinesin-1 and dynein association with axonal vesicles. *Proc. Natl. Acad. Sci. USA*, **109**, 8582–8587.
29. Stadler, C., Rexhepaj, E., Singan, V.R., Murphy, R.F., Pepperkok, R., Uhlen, M., Simpson, J.C. and Lundberg, E. (2013) Immunofluorescence and fluorescent-protein tagging show high correlation for protein localization in mammalian cells. *Nat. Methods*, **10**, 315–323.
30. Goldsbury, C., Mocanu, M.M., Thies, E., Kaether, C., Haass, C., Keller, P., Biernat, J., Mandelkow, E. and Mandelkow, E.M. (2006) Inhibition of APP trafficking by tau protein does not increase the generation of amyloid-beta peptides. *Traffic*, **7**, 873–888.
31. Gibson, T.J., Seiler, M. and Veitia, R.A. (2013) The transience of transient overexpression. *Nat. Methods*, **10**, 715–721.
32. Berkenbosch, F., Refolo, L.M., Friedrich, V.L. Jr, Casper, D., Blum, M. and Robakis, N.K. (1990) The Alzheimer's amyloid precursor protein is produced by type I astrocytes in primary cultures of rat neuroglia. *J. Neurosci. Res.*, **25**, 431–440.
33. Refolo, L.M., Wittenberg, I.S., Friedrich, V.L. Jr and Robakis, N.K. (1991) The Alzheimer amyloid precursor is associated with the detergent-insoluble cytoskeleton. *J. Neurosci.*, **11**, 3888–3897.
34. Adams, S.R., Campbell, R.E., Gross, L.A., Martin, B.R., Walkup, G.K., Yao, Y., Llopis, J. and Tsien, R.Y. (2002) New biarsenical ligands and tetracysteine motifs for protein labeling in vitro and in vivo: synthesis and biological applications. *J. Am. Chem. Soc.*, **124**, 6063–6076.
35. Whitmarsh, A.J., Cavanagh, J., Tournier, C., Yasuda, J. and Davis, R.J. (1998) A mammalian scaffold complex that selectively mediates MAP kinase activation. *Science*, **281**, 1671–1674.
36. Borg, J.P., Ooi, J., Levy, E. and Margolis, B. (1996) The phosphotyrosine interaction domains of X11 and FE65 bind to distinct sites on the YENPTY motif of amyloid precursor protein. *Mol. Cell. Biol.*, **16**, 6229–6241.
37. Qi, Y., Wang, J.K., McMillian, M. and Chikaraishi, D.M. (1997) Characterization of a CNS cell line, CAD, in which morphological differentiation is initiated by serum deprivation. *J. Neurosci.*, **17**, 1217–1225.
38. Lee, M.S., Kao, S.C., Lemere, C.A., Xia, W., Tseng, H.C., Zhou, Y., Neve, R., Ahlijanian, M.K. and Tsai, L.H. (2003) APP processing is regulated by cytoplasmic phosphorylation. *J. Cell Biol.*, **163**, 83–95.
39. Muresan, V. and Muresan, Z. (2012) A persistent stress response to impeded axonal transport leads to accumulation of amyloid-beta in the endoplasmic reticulum, and is a probable cause of sporadic Alzheimer's disease. *Neuro-Degener. Dis.*, **10**, 60–63.
40. Muresan, Z. and Muresan, V. (2004) A phosphorylated, carboxy-terminal fragment of β-amyloid precursor protein localizes to the splicing factor compartment. *Hum. Mol. Genet.*, **13**, 475–488.
41. Muresan, Z. and Muresan, V. (2005) c-Jun NH2-terminal kinase-interacting protein-3 facilitates phosphorylation and controls localization of amyloid-beta precursor protein. *J. Neurosci.*, **25**, 3741–3751.
42. Muresan, Z. and Muresan, V. (2006) Neuritic deposits of amyloid-β peptide in a subpopulation of central nervous system-derived neuronal cells. *Mol. Cell. Biol.*, **26**, 4982–4997. PMCID: PMC1489158.
43. Muresan, Z. and Muresan, V. (2007) The amyloid-β precursor protein is phosphorylated via distinct pathways during differentiation, mitosis, stress, and degeneration. *Mol. Biol. Cell*, **18**, 3835–3844. PMCID: PMC1995701.
44. Muresan, Z. and Muresan, V. (2009) CAD cells are a useful model for studies of APP cell biology and Alzheimer's disease pathology, including accumulation of Aβ within neurites. SWAN Alzheimer knowledge base. *Alzheimer Res. For*. Available at: http://hypothesis.alzforum.org/swan/browser/showEntity.action?ObjectId=urn:lsid:swan.org:researchstatement:ca7169f1-ff7d-456c-b3f3-c52bec1e8074, last accessed on 29 December 2009.
45. Park, Y.U., Jeong, J., Lee, H., Mun, J.Y., Kim, J.H., Lee, J.S., Nguyen, M.D., Han, S.S., Suh, P.G. and Park, S.K. (2010) Disrupted-in-schizophrenia 1

(DISC1) plays essential roles in mitochondria in collaboration with Mitofilin. *Proc. Natl. Acad. Sci. USA*, **107**, 17785–17790.
46. Braak, H. and Del Tredici, K. (2012) Where, when, and in what form does sporadic Alzheimer's disease begin? *Curr. Opin. Neurol.*, **25**, 708–714.
47. Braak, H., Thal, D.R., Ghebremedhin, E. and Del Tredici, K. (2011) Stages of the pathologic process in Alzheimer disease: age categories from 1 to 100 years. *J. Neuropathol. Exp. Neurol.*, **70**, 960–969.
48. Muresan, Z. and Muresan, V. (2008) Seeding neuritic plaques from the distance: a possible role for brainstem neurons in the development of Alzheimer's disease pathology. *Neuro-Degener. Dis.*, **5**, 250–253. PMCID: PMC2562573.
49. Braak, H. and Braak, E. (1991) Neuropathological stageing of Alzheimer-related changes. *Acta Neuropathol. (Berl).*, **82**, 239–259.
50. Tan, J., Mao, G., Cui, M.Z., Lamb, B., Sy, M.S. and Xu, X. (2009) Residues at P2-P1 positions of epsilon- and zeta-cleavage sites are important in formation of beta-amyloid peptide. *Neurobiol. Dis.*, **36**, 453–460.
51. Tan, J., Mao, G., Cui, M.Z., Kang, S.C., Lamb, B., Wong, B.S., Sy, M.S. and Xu, X. (2008) Effects of gamma-secretase cleavage-region mutations on APP processing and Abeta formation: interpretation with sequential cleavage and alpha-helical model. *J. Neurochem.*, **107**, 722–733.
52. Muresan, Z. and Arvan, P. (1997) Thyroglobulin transport along the secretory pathway. Investigation of the role of molecular chaperone, GRP94, in protein export from the endoplasmic reticulum. *J. Biol. Chem.*, **272**, 26095–26102.
53. Muresan, V., Abramson, T., Lyass, A., Winter, D., Porro, E., Hong, F., Chamberlin, N.L. and Schnapp, B.J. (1998) KIF3C and KIF3A form a novel neuronal heteromeric kinesin that associates with membrane vesicles. *Mol. Biol. Cell*, **9**, 637–652.
54. Zar, J.H. (1999) *Biostatistical Analysis*. Prentice Hall, Upper Saddler River, NJ.
55. Nikolaev, A., McLaughlin, T., O'Leary, D.D. and Tessier-Lavigne, M. (2009) APP binds DR6 to trigger axon pruning and neuron death via distinct caspases. *Nature*, **457**, 981–989.